Badia, J. D., Strömberg, E., Karlsson, S., & Ribes-Greus, A. (2012). Material valorisation of amorphous polylactide. Influence of thermo-mechanical degradation on the morphology, segmental dynamics, thermal and mechanical performance. *Polymer degradation and stability*, *97*(4), 670-678.

MATERIAL VALORISATION OF AMORPHOUS POLYLACTIDE. INFLUENCE OF THERMO-MECHANICAL DEGRADATION ON THE MORPHOLOGY, SEGMENTAL DYNAMICS, THERMAL AND MECHANICAL PERFOMANCE

J.D. Badia[1], E. Strömberg[2], S. Karlsson[2,3], A. Ribes-Greus[1,*]

DOI: https://doi.org/10.1016/j.polymdegradstab.2011.12.019

Please, cite it as:

Badia, J. D., Strömberg, E., Karlsson, S., & Ribes-Greus, A. (2012). Material valorisation of amorphous polylactide. Influence of thermo-mechanical degradation on the morphology, segmental dynamics, thermal and mechanical performance. *Polymer degradation and stability*, *97*(4), 670-678.

[1] Instituto de Tecnología de Materiales (ITM),

Universitat Politècnica de València

Camino de Vera s/n, E-46022 Valencia, Spain

[2] School of Chemical Science and Engineering,

Fibre and Polymer Technology,

KTH - Royal Institute of Technology,

Teknikringen 56-58, SE-10044 Stockholm, Sweden

[3]Presently, Vice Chancellor Skövde University, SE-541 28 SKÖVDE, Sweden

*corresponding author: A. Ribes-Greus

aribes@ter.upv.es

Badia, J. D., Strömberg, E., Karlsson, S., & Ribes-Greus, A. (2012). Material valorisation of amorphous polylactide. Influence of thermo-mechanical degradation on the morphology, segmental dynamics, thermal and mechanical performance. *Polymer degradation and stability*, *97*(4), 670-678.

MATERIAL VALORISATION OF AMORPHOUS POLYLACTIDE. INFLUENCE OF THERMO-MECHANICAL DEGRADATION ON THE MORPHOLOGY, SEGMENTAL DYNAMICS, THERMAL AND MECHANICAL PERFOMANCE

J.D. Badia[1], E. Strömberg[2], S. Karlsson[2,3], A. Ribes-Greus[1,*]

[1] Instituto de Tecnología de Materiales (ITM),

Universitat Politècnica de València

Camino de Vera s/n, E-46022 Valencia, Spain

[2] School of Chemical Science and Engineering,

Fibre and Polymer Technology,

KTH - Royal Institute of Technology,

Teknikringen 56-58, SE-10044 Stockholm, Sweden

[3] Presently, Vice Chancellor Skövde University, SE-541 28 Skövde, Sweden

*corresponding author: A. Ribes-Greus

aribes@ter.upv.es

Badia, J. D., Strömberg, E., Karlsson, S., & Ribes-Greus, A. (2012). Material valorisation of amorphous polylactide. Influence of thermo-mechanical degradation on the morphology, segmental dynamics, thermal and mechanical performance. *Polymer degradation and stability*, *97*(4), 670-678.

MATERIAL VALORISATION OF AMORPHOUS POLYLACTIDE. INFLUENCE OF THERMO-MECHANICAL DEGRADATION ON THE MORPHOLOGY, SEGMENTAL DYNAMICS, THERMAL AND MECHANICAL PERFOMANCE.

J.D. Badia[1], E. Strömberg[2], S. Karlsson[2,3], A. Ribes-Greus[1,*]

Keywords: poly(lactide) (PLA), material valorisation, mechanical recycling, thermo-mechanical degradation, cold-crystallization, segmental dynamics

Abstract:

This paper reports the effects of multiple mechanical recycling on the structure and properties of amorphous polylactide (PLA). The influence of the thermo-mechanical degradation induced by means of five successive injection cycles was initially addressed in terms of macroscopic mechanical properties and surface modification. A deeper inspection on the structure and morphology of PLA was associated to the thermal properties and viscoelastic behaviour. Despite the FTIR analysis did not show significant changes in functional groups, a remarkable reduction in molar mass was found by viscosimetry. PLA remained amorphous throughout the reprocessing cycles, but the occurrence of a cold-crystallization during DSC and DMTA measurements, which enthalpy increased with each reprocessing step, suggested chain scission due to thermo-mechanical degradation. The effect of chain shortening studied on the glass-rubber relaxation by DMTA showed an increase in free-volume affecting the segmental dynamics of PLA, particularly after the application of the second reprocessing step, in connection to the overall loss of performance showed by the rest of properties.

1. Introduction

The interest on plastic materials such as poly (lactic acid)s or polylactides (PLA) that accomplish the two-fold benefit of being biodegradable and come from renewable resources has gained much attention. Polylactides are thermoplastic polyesters obtained from the ring-opening polymerization of lactide, which may be derived from the fermentation of sugar feedstocks at competitive prices compared to that previously achievable from petrochemical-derived products [1]. PLAs have numerous interesting properties including good processability, mechanical properties, thermal stability and low environmental impact [2-3], which enhance their performance as suitable candidates for replacing commodities at the packaging sector. Indeed, the application of life cycle assessments [4] has shown that the use of PLA in common polymeric fossil-based applications performs environmentally better, in terms of a lower use of fossil energy, a reduced emission of greenhouse gases and for being a great source of carbon after disposal. However, the increase of a new source of polymeric waste is implied, which would have to be managed. Moreover, with the aim of enhance the material valorisation of PLA goods, it would be advisable to explore the possibilities of extending their service lives before finally discarding them to bio-disposal facilities, such as composting plants. Among all material recovery methods [5], mechanical recycling represents one of the most successful processes and has received considerable attention due to its main advantages, since it is relatively simple, requires low investment, and its technological parameters are controlled. Nevertheless, polymers are subjected to the influence of degrading agents such as oxygen, UV-light, mechanical stresses, temperature and water, which, separately or in combination, during its material loop (synthesis - processing - service life - discarding - recovery), results in chemical and physical changes that alter their stabilization mechanisms and long-term properties . These degradation processes may modify the structure and composition of PLA and consequently change the thermal, viscoelastic and mechanical properties of the recyclates [6].

On the one hand, the simulation of mechanical recycling by multiple processing and service life by accelerated thermal ageing to assess the effects of thermal and thermo-mechanical degradation has been previously performed for commodities [6-17]. Studies on the degradation of reprocessed PLA report the influence of multiple extrusion [18] or injection cycles [19-22], as well as different sets of combined individual cycles of

extrusion, injection and annealing [23-24] on the chemical structure, oligomeric distribution, morphology, thermal, rheological, mechanical or permeability properties. The features of processed PLA strongly depend on its stereochemistry and thus the impact of the proportion of L- and D- enantiomers is a matter of continuous work in literature [25]. Previous studies reported the apparition of a crystalline phase after a certain number of processing cycles for a PLA with 8% D-content [19] which influenced the performance of PLA due to decoupling of amorphous and crystalline phases and consequently acted as a topological constraint decreasing chain mobility and modifying the mechanical properties with further processing. Concerning studies on PLA with D-content similar to the PLA used in this study (4.25%), no formation of crystalline phase was found during one cycle of injection or extrusion. However, an annealing step triggered the formation of crystalline domains thus affecting the mechanical properties of the material. In contrasts, this study reports the performance of reprocessed PLA which remained amorphous regardless the number of processing cycles.

The purpose of this work was therefore to characterize the influence of multiple processing on PLA microstructure, and its subsequent influence on its thermal and mechanical performance, as well as in segmental dynamics, as a means for modelling mechanical recycling as a suitable valorisation option for recovering PLA prior to bio-disposal.

2. Experimental procedure

2.1. Material and reprocessing simulation

Polylactide (PLA) 2002D, which contain 4.25% mol of D-lactic enantiomer and has a density of 1.24 g/cm3, according to manufacturer [26] was a thermo-forming grade PLA obtained from Natureworks LLC (Minnetonka, MN) as pellets, provided by AIMPLAS (Paterna, Spain). Prior to processing, virgin PLA pellets were dried during 2 h at 80 ºC in a dehumidifier Conair Micro-D FCO 1500/3 (UK), in order to remove as much humidity as possible from PLA flakes. Afterwards, the samples were processed by means of injection moulding by means of an Arburg 420 C 1000-350 (Germany) injector, single-screw model (diameter Φ=35 mm, length/Φ=23). Temperature gradient set from hopper to nozzle was 160, 170, 190, 200 and 190ºC. Moulds were set at 15 ºC. Cooling time residence was ~ 40 s and total residence time ~ 60s. Samples were dried before each

processing cycle. After injection, a fraction of the samples was kept as test specimens and the rest was ground by means of a cutting mill Retsch SM2000 (UK), which provided pellets of size d< 20 mm to be fed back into the process. Up to five processing cycles were applied under the same conditions to obtain the different testing specimens of reprocessed PLA (RPLA-i, with i: 1-5). Dumbbell probes for tensile and impact testing were obtained according to ISO 527-2 (type 1A) [27]. 1 mm thick prismatic probes for SEM and DMTA were obtained from compression moulding, as described elsewhere [28].

2.2. Mechanical properties

Tensile testing and impact testing were carried out at laboratory conditions 23/50, according to ISO 291, atmosphere 23/50, class 1 [29]. Tensile tests were performed on reprocessed PLA in order to investigate the changes in macroscopic mechanical properties, by means of an Instron 5566 universal electromechanical testing instrument (Instron Corp, MA, USA), at a crosshead speed of 5 $mm \cdot min^{-1}$, a 10 kN load cell and gauche length of 50 mm. Analyses were repeated at least 6 times per material, and the average of elastic modulus, elongation at break and stress at break were used as representative values.

Charpy impact experiments were carried out following ISO 179 [30], with a hammer of 1 J and a notch size radius of 1,5mm. The samples were characterized at least by triplicate and the averages were taken as representative values.

2.3. Scanning Electron Microscopy (SEM)

The morphology of the specimens was analysed by means of a Hitachi S-4800 Field Emission Scanning Electron Microscope (Tokyo, Japan). The samples from each material were prepared by cutting square pieces from a randomly chosen part of the processed specimen. The pieces were mounted on metal studs and sputter-coated with a 2 nm gold layer using a Cressington 208HR high resolution sputter coater (Watford, UK), equipped with a Cressington thickness monitor controller.

2.4. Differential Scanning Calorimetry (DSC)

DSC analyses were carried out by a Mettler Toledo DSC 820 instrument (Columbus, OH) calibrated with indium and zinc standards. Approximately 5 mg of

pellets were placed in 40 μL aluminium pans, which were sealed and pierced to allow the N_2 gas flow (50 ml·min^{-1}). A heating/cooling/heating program with a +/- 2ºC·min^{-1} rate was employed in the temperature range between 0 ºC and 200 ºC. The samples were characterized at least by triplicate and the averages were taken as representative values.

2.5. Fourier-Transform Infrared (FT-IR) Analysis

FT-IR spectra were collected by a NEXUS Thermo Nicolet 5700 FT-IR Spectrometer (MA, USA), previously calibrated, and equipped with a single-reflection Smart Performer accessory for attenuated total reflection (ATR) measurements, with diamond crystal. 32 co-added spectra were recorded for each specimen at a resolution of 4 cm^{-1} with a spacing of 1 cm^{-1}, from 4000 to 600 cm^{-1} of wavenumber. Spectra were normalized to the 1454 cm^{-1} peak [31] before any data processing which is usually used as internal standard and it is useful to correct possible variations arisen from defects in surface quality or sample positioning. At least 8 measurements per material were performed, in order to obtain representative results. Presented spectra correspond to the average of each individual analysis.

2.6. Viscosimetry

The intrinsic viscosity $[\eta]$ was measured according to the standard ISO 1628-1 [32], by means of a Cannon-Fleske capillary viscosimeter type at 30 ºC, with the use of analytical grade tetrahydrofurane (THF) supplied by Fluka as solvent. Dissolutions of pellets ranged from 0.1 to 1 g·dL^{-1}.Measurements were performed by quintuplicate for each concentration c and $[\eta]$ was obtained from extrapolation to $c \rightarrow 0$ of Huggins and Kraemer plots, which respectively account for the variation of reduced η_{red} and inherent η_{inh} viscosities with the concentration c, being $\eta_{red} = c^{-1} \cdot \eta_{sp}$, $\eta_{inh} = c^{-1} \cdot \ln \eta_{rel}$, $\eta_{sp} = \eta_{rel} - 1$ and $\eta_{rel} = t \cdot t_0^{-1}$, where t and t_0 were the times (s) of flowing of the dissolution and solvent, respectively. The viscous molar mass values (M_V, g·mol^{-1}) was calculated with the Mark-Houwink equation $[\eta] = K \cdot M_V^{\alpha}$, with constants $K = 6.4 \cdot 10^{-4}$ dL·g^{-1} and $\alpha = 0.68$ [33].

2.7. Dynamical-Mechanical Thermal Analysis (DMTA)

DMTA test were conducted in dual cantilever clamping with 15 mm of effective length between clamps, with the three point bending mode, by means of a DMA/SDTA861^e Dynamic Mechanical Analyzer, from Mettler-Toledo (OH, USA).

Experiments were carried out from 25 ºC to 130 ºC with isothermal steps of 2ºC, measuring 24 frequencies (8 per decade) between 0.1 and 100 Hz. Analyses were performed at least thrice per sample and the average was taken as representative values.

2.8. Analytical software and computational assumptions.

FT-IR spectra were characterized by OMNIC 7.0 from Thermo Scientific. DSC and DMTA analyses were performed with the aid of the software STAR^e 9.10 from Mettler-Toledo. Fitting procedures were performed by means of OriginLab OriginPro 8.0, which uses the Levenberg-Marquardt algorithm [34-35] to adjust the parameter of the fitting values in the iterative procedure.

Values are plotted in terms of {average, dev_{max}, dev_{min}}, where dev_{max} = max(data)-average(data), and dev_{min} = average (data)-min(data). Tabulated errors correspond to the standard deviation of data.

3. Results and discussion

3.1. Surface characterization and mechanical performance

The surface characterization of reprocessed PLA by SEM, shown in **Figure 1** exhibited typical topologies of industrially-processed polymers [7,9]. After 5 reprocessing cycles, the micrographs presented a rough and heterogeneous surface where inefficiently melted particles arose, in comparison to that of VPLA, anticipating modifications in the performance of the material. The effects of reprocessing on the macroscopic mechanical properties are shown in **Figure 2**, in terms of Young modulus, stress and strain at break and impact value. The Young modulus remained almost unaltered during the 2 first reprocessing cycles, which was in agreement with previous reports in which this PLA grade showed similar performance [23]. However, from the third injection cycle on, the Young modulus decreased showing a significant drop (~ 28 %) for the fifth recyclate. On the other hand, the impact resistance was decreased by ~ 10% after the first cycle, maintaining its value nearly invariant throughout the rest of injections, as comparable with the behaviour shown by multi-extruded PLA [18]. The strain at break showed an overall increasing fashion within a narrow range, i.e. a ~ 21 % from VPLA to RPLA-5. However, the values were still very low in contrast to other plastics used in packaging, such as PET [14]. On the other hand, a small and gradual drop in the stress at break values (~ 6,6 %) was also presented. The diminution of mechanical performance along the reprocessing cycles could be attributed to the inherent chain scission processes [20]. However, the rearrangement of chains in the matrix may affect the final properties. Indeed, the macroscopic mechanical results differ significantly from those reported elsewhere for PLA with higher D- content [19], which showed higher reductions in strain and stress at break, which were attributed to the formation of crystalline fractions that might favour the crack propagation in the amorphous domain. On the contrary, the results are in agreement with those reported for the same PLA grade [23], where no crystalline fraction was found after injection or extrusion. Further analytical characterization helped assess the type of chain rearrangement after the thermo-mechanical degradation induced by multiple processing.

Figures 1-2

3.2. Structural changes

The absorbance spectra of virgin polylactide (VPLA) and its successive recyclates were recorded by Fourier-Transform Infrared Spectroscopy (FT-IR), as shown in **Figure 3a** for the case of VPLA and RPLA-5. The spectra of intermediate RPLA-i were similar. Complete description of the bands can be found in literature [31]. In a previous study carried out by means of MALDI-TOF MS analyses [20], the presence of new carboxy-methyl and carboxyl terminated species underwent by reprocessing was reported. In order to ascertain a semi-quantitative picture of the structural changes caused by reprocessing, the relative absorbance ratios of the areas corresponding to the maximum peaks of the C-H stretching region (3100-2800 cm^{-1}, **Figure 3c**), and the maxima of the C=O stretching region (1800-1700 cm^{-1} **Figure 3b**) were determined related to the area of the reference peak at 1454 cm^{-1} which is assigned to the C-H asymmetric bending mode and known to be suitable as internal standard [31], to obtain comparable results without experimental influence of the dimensions of the probes. Both functional indexes (**Figure 3d)** showed an increasing tendency, more significant for the carbonyl group, along with a displacement to higher wavenumbers of the peak, which may be indicative of the appearance of new carbonyl-linked species both in the middle and at the end as carboxyl groups, and may be a symptom of reduction of molar mass.

Consequently, the viscous molar mass (M_V) was assessed and its evolution correlated to the number of reprocessing cycles, as shown in **Figure 4**. The linear regression values obtained for both Huggins and Kraemer plots for all materials were higher than 0.975. The inset in **Figure 4** shows an example of both plots for the case of VPLA. The M_V decreased steeply with each reprocessing step, with marginal drops around 10 % until the third recyclate and bigger ones afterwards. After 5 reprocessing cycles, a 50 % decrease of M_V ranged from VPLA to RPLA-5. These results indicated a sort of threshold for the structure to resists further thermo-mechanical degradation until 2 reprocessing cycles. Consequently, the macroscopic mechanical performance might be affected, as previously observed. In the next sections, these changes were studied in terms of calorimetric parameters and segmental dynamics.

Figures 3-4

3.3. The study of the amorphous and crystalline phases of reprocessed PLA.

The cooling scans of VPLA and its further recyclates uniquely showed a glass transition, thus suggesting that reprocessing did not promoted the apparition of a crystalline phase. This was confirmed by FT-IR analysis, which showed that there was no generation of new bands at 687, 739, 921 and 1293 cm^{-1}, representative of crystalline regions along the reprocessing cycles [31].

However, the heating scans displayed, besides the glass transition, a cold-crystallization and a subsequent melting, as shown in **Figure 5** for all materials. The calorimetric thermograms were characterized by the key indicators in each region:

(i) the glass transition temperature (T_G) was calculated as the temperature at the midpoint, according to ISO 11357-2 [36];
(ii) the cold-crystallization induced by the DSC temperature program was characterised by the induction and peak temperatures (T_{CC0} and T_{CC}, respectively), and the specific cold-crystallization enthalpy (Δh_{CC}), which represents the area between the baseline and the exothermic curve;
(iii) the melting of the cold-crystallized domains was assessed by the peak temperature (T_M) and the area between baseline and the endotherm, from which the specific melting enthalpy (Δh_M) was obtained.

The variation of these parameters can be seen at **Table 1**. A low reduction of T_G was observed, which may be related to an increase of free volume due to the presence of more end chains and a consequent molar mass reduction. According to the Fox-Flory relationship [37], this small variation could indicate that the decrease of molar mass induced by reprocessing was not significant enough to dramatically reduce the T_G. Concerning the evolution of T_{CC0} and T_{CC}, a progressive diminution was shown along the successive reprocessing cycles. In addition, a significant increment in Δh_{CC} was found from VPLA to the first recyclate, to nearly equal values until the last injection cycle. The same trend was found for Δh_M. Quantitatively, it was proved that $\Delta h_M \sim \Delta h_{CC}$ for both virgin and reprocessed PLAs, which meant that all the crystalline domains produced during the cold-crystallization were completely melted. The chain scission due to thermo-mechanical degradation may lead to shorter chains acting as nucleation centres, thus increasing the Δh_{CC} and then modifying the crystallization kinetics and consequently the

processability of PLA [38]. All these results were in contrast to those reported in other studies with a PLA with a 8% of D- content and $22 \cdot 10^4$ g·mol^{-1} of molar mass, which showed a drop of T_G of about 10 ºC and the presence of crystalline phases in the glassy state, which appeared during cooling. Interestingly, this formation of crystalline domains was reported after the second injection cycle [19].

A deep characterisation of the melting behaviour of these newly formed crystallites was necessary to shed light on the influence of thermo-mechanical degradation. The shape of the endotherms showed a change from a uni-modal to a bi-modal distribution, which might be attributed to a superimposed melting-crystallization-melting process, dependant on the kinetics of the temperature program [39-40].

In order to extent the study of the DSC bimodal melting, a deconvolution procedure [28] was applied to describe both processes individually. The fit correlation values R^2 were higher than 0.952. A partial areas study [10] allowed monitoring the evolution of both crystalline domains as given at **Figure 6**, in terms of peak temperatures ($T_M{}^i$) and relative partial areas ($A_M{}^i$), where i=I or II were used as labels for the lowest and highest peak temperatures, respectively. It could be seen how both parameters behaved likewise in pairs, describing similar decreasing or increasing profiles. The peaks were separated progressively until the second recyclate, where the position of the endotherms, characterized by its peak temperature, held unmovable for the rest of recyclates. Simultaneously, $A_M{}^I$ decreased progressively reaching almost equal proportions than of $A_M{}^{II}$. The effect of the thermo-mechanical degradation could be ascribed to the variation of the first area $A_M{}^I$, which would be indicative of the promoted tendency of crystals to melt, and thus for molten shorter chains to recrystallize. Both overall decreases of ~5 ºC in $T_M{}^I$ and ~ 47 % in $A_M{}^I$ suggested the presence of weaker cold-crystallized domains along the injection cycles. The stabilization of $T_M{}^I$ after the second reprocessing step may suggest the homogenization of size of the scissored chains to a limiting length. In addition, the increase of $A_M{}^I$ may indicate the continuation of the chain scission processes of previously uncut chains during further reprocessing cycles. The arrangement of these shorter chains in terms of mobility might be the indicators for the variations in the mechanical properties shown at the beginning of the study. Hence, the cooperative movement of PLA chains was investigated by DMTA.

Figures 5-6, Table 1

3.4. Viscoelastic behaviour and segmental dynamics

The assessment of the glass-rubber relaxation and the segmental dynamics of PLA has been reported in several studies [41-43] for different PLA grades, but not shown for the case of reprocessed PLA. **Figure 7** shows the isochronal plots of the storage (*E'*) and loss (*E''*) moduli versus temperature for virgin PLA at the commonly used frequency of 1 Hz. Similar curves were obtained for all the other frequencies, but they are not displayed to avoid visualization matters.

Figure 7

The viscoelastic spectra showed different relaxation zones which were related to the calorimetric transitions along the increasing temperature-axis. At temperatures reaching the glass-rubber relaxation, the PLAs showed a drop in the storage modulus of nearly 99% of the initial value that after a rubbery plateau increased until 5-8 % of the modulus was recovered by the formation of crystalline phases in the rubber state, regardless the reprocessing cycle or frequency analysed. The influence of reprocessing can be observed in **Figure 8**, where the DMTA scans of recyclates are shown in comparison with those of VPLA. The parameters used for characterisation were temperature gradients ($\Delta T'_{RP}$, $\Delta T'_{RC,}$ $\Delta T''_{GR}$, and $\Delta T''_{RC}$) and mechanical stresses ($\Delta E'_{GR}$, $\Delta E'_{RC,}$ $\Delta E''_{0}$, $\Delta E''_{GR}$, and $\Delta E''_{RC}$) where the subscripts *0*, *GR*, RP and *RC* stand for initial, glass-rubber transition, rubbery plateau, and recrystallization, respectively. The values averaged from the experiments at all frequencies are given in **Table 2**.

All the temperature gradients showed a decreasing profile. Concerning the evolution of $\Delta T'_{RP}$, a widening of the rubbery plateau due to the addition of chemical cross-linkers to PLA was reported elsewhere [44]. Conversely, the shortening of the rubbery plateau registered in **Table 2** might be indicative of chain cleavage. Likewise, the decrease in $\Delta T'_{RC}$ was related to the presence of shorter chains after each reprocessing cycle, which would speed up the nucleation inducing a cold-crystallization at lower temperatures, as also shown by the DSC results (T_{CC0}). Regarding the evolution of the mechanical stresses, an initial increase up to the second recyclate was shown, and afterwards the values decreased to nearly equal values for RPLA-3,4,5. The origin of these results can be understood in terms of cooperative movement within the amorphous phase throughout

the glass-rubber relaxation and thus a deeper inspection into the influence of reprocessing into the glass-forming behaviour of PLA was performed.

F*igure 8 - Table 2*

Shortly, a fragile glass-former experiences a dramatic loss of properties (rheological, mechanical…) throughout a specific short temperature interval, such as the glass-rubber relaxation, while a strong glass-former maintains its properties without any significant change. The relaxation of strong systems is generally found to be Arrhenius like, whereas for fragile systems, it is remarkably non-Arrhenius [45-46] and describable by a Vogel-Fulcher-Tamman-Hesse (VFTH) behaviour [47-49] , as shown in Eq. (1)

$$\tau(T) = \tau_0 \cdot exp\left(\frac{B}{T - T_{VFTH}}\right) = \tau_0 \cdot exp\left(\frac{D \cdot T_{VFTH}}{T - T_{VFTH}}\right)$$

(1)

, where τ are the relaxation times (s), that is (2·π·f)-1, and f is the linear frequency of the DMTA tests, τ0 is a time reference scale, and B (K) and TVFTH (K) are positive parameters specific to the material. TVFTH typically appears 40-60 K below the TG. It is common to rewrite the parameter B into B = D· TVFTH, where D is a dimensionless factor termed as fragility or strength parameter. Qualitatively, D is related to the topology of the theoretical potential energy surface of the system, where fragile systems (D ≤ 6) present high density of energy minima, contrarily to strong systems (D≥15) which present lower density. As well, the so-called fragility index m permits an assessment of the deviation of τ(T) from the Arrhenius behavior of polymers. It varies between two limiting values of 16 and ≥ 200 for strong and fragile glass-formers, respectively [50], and can be obtained by the following expression:

$$m = \left.\frac{d\ \log\ (\tau)}{d(T_G/T)}\right|_{T=TG} = \left.\frac{B \cdot T}{\ln(10) \cdot (T_G - T_{VFTH})^2}\right|$$

(2)

In order to study the effects of reprocessing on the dynamic fragility of PLA, the relationship of τ with the TP from the different loss tangent spectra were fitted to the

VFTH model, which results with linear correlation R2 coefficients higher than 0,950 are gathered in **Table 3**, along with the fragility parameters D, B and m. VPLA showed fragile glass-former performance, in agreement with other studies performed on fully amorphous PLA [51]. Up to the second recyclate, PLA became more fragile. Afterwards, there was a change in the variation trend. These results were in agreement with the evolution shown by the mechanical stresses, as can be seen in **Table 2.** The influence of the chemical structure of polymers on their fragility was discussed with detail by Sokolov et al. [52]. The changes can be ascribed to the mobility of chains, both physically or chemically, which in turn will affect the cooperative movement and the packing efficiency. An increase in fragility implies higher chain cooperativity and vice versa. Thus, the subsequent calculation of the activation energies related to the glass-rubber relaxation EaGT, or the free volume coefficient obtained by means of Eqs. (3) and (4) could picture the change in cooperative movement due to thermo-mechanical degradation.

$$Ea_{GT} = R \cdot \frac{d\ln\tau}{d\left(1/T\right)} = \frac{R \cdot B}{\left(1 - \frac{T_{VFTH}}{T}\right)^2} \quad (3)$$

$$\phi = \frac{(T - T_{VFTH})}{B} \quad (4)$$

As can be seen in **Figure 9**, both parameters displayed a logical contrary behaviour. After the second recyclate, the free volume considerably increased (~20 %) which may promote the liability of gases to permeate through the packing defects of the polymer in packaging applications therefore reducing the second-life performance of PLA for similar purposes.

Table 3-Figure 9

3.5. Summary of results

The thermo-mechanical degradation inherent to mechanical recycling induced chain scission reactions releasing mainly carboxyl species which remained amorphous regardless the number of injection cycles. Consequently, the viscous molar mass decayed. Chain scission could be followed by monitoring the col-crystallization induced during the

calorimetric experiments, in terms of a decrease of the cold-crystallization temperature and an increase in the cold-crystallization enthalpy. The tendency of the bimodal melting endotherm to change towards the peak at lower temperatures TM I, along with the stabilization of the partial melting temperature just after the second reprocessing step may indicate that a limiting length of scissored chain was attained.

The arrangement of the scissored chains in the amorphous matrix was noticeably influent from the second reprocessing step on. The reduction of chain length during further injection cycles might had affected the mobility of chains leaving more free volume, thus easing the glass-rubber relaxation with lower mechanical stresses and activation energies, since the dynamic fragility was reduced. In connection, the less efficient packing of PLA reprocessed more than 2 times could explain the reduction of the Young Modulus and stress at break found in the study of the macroscopic mechanical properties.

4. Conclusions

Polylactide (PLA) submitted to in-plant recycling simulation underwent thermomechanical degradation which modified its structure and morphology and induced changes on its thermal and mechanical properties. Despite non-significant changes were drawn from the observation of the functional groups of PLA, a remarkable reduction in molar mass was found, due to chain scission processes After each of the 5 applied reprocessing steps, PLA remained amorphous in the glassy state. However, the study of the calorimetric thermograms showed the apparition of a cold- crystallization phenomenon, which was favoured by the presence of shorter PLA chains due to chain scission processes, particularly after the second reprocessing cycle. This fact was also confirmed by monitoring the melting endotherm. The rearrangement of cut chains into the amorphous matrix offered more free volume which favoured the mobility of chains throughout the glass-rubber relaxation and reduced the dynamic fragility of reprocessed PLA. In macroscopic terms, it was related to a decay in elastic modulus and stress at break, as well as it influenced the surface heterogeneity.

As a whole, all assessed properties showed a significant loss of PLA performance after the application of the second reprocessing step, thus suggesting a sort of threshold to be recovered by further mechanical recycling.

Acknowledgements

The authors would like to acknowledge the Spanish Ministry of Science and Innovation for the financial support through the Research Project UPOVCE-3E-013 and for the funding of a predoctoral research position to J.D. Badía by means of the FPU program conceded by the Spanish Ministry for Education. The authors acknowledge the financial support of the Generalitat Valenciana through the ACOMP/2011/189. Universitat Politècnica de València (UPV, Spain) is thanked for additional support through the PAID 05-09-4331 program and Royal Institute of Technology (KTH, Sweden) is thanked for additional. Mr. Enrique Benavent at AIMPLAS is acknowledged for taking care of processing the material. Mr. Peter Kaali at KTH is thanked for carrying out impact tests and Mrs. Sevil Atari Jabarzadeh at KTH for helping with SEM analysis. Mrs. L. Santonja-Blasco at UPV is thanked for endless and enjoyable discussions.

References

1. Mohanty AK, Misra M, Hinrichsen G. Biofibres, biodegradable polymers and biocomposites: an overview. Macromolecular Materials and Engineering 2000; 276: 1-24

2. Tsuji H, Doi Y. Biopolymers. Polyesters III. Applications and commercial Products. In: Steinbüchel A, editor. Biopolymers. Weinheim : Wiley-VCH Verlag GMbh, 2002.

3. Auras R, Harte S, Selke S. An overview of polylactides as packaging materials. Macromolecular Bioscience 2004; 4: 835-865.

4. Vink E T H, Rábago K R, Glassner D A, Gruber P R. Applications of life cycle assessment to NatureWorks™ polylactide (PLA) production. Polymer Degradation and Stability, 2003; 80: 403-419.

5. Al-Salem S M, Lettieri P, Baeyens J. Recycling and recovery routes of plastic solid waste (PSW): A review. Waste management 2009;29: 2625-2643.

6. Vilaplana F, Karlsson S. Quality concepts for the improved use of recycled polymeric materials: a review. Macromolecular Materials and Engineering 2008; 293: 274-297.

7. Strömberg E, Karlsson S. The design of a test protocol to model the degradation of polyolefins during recycling and service life. Journal of Applied Polymer Science 2009; 112: 1835-1844.

8. Vilaplana F, Ribes-Greus A, Karlsson S. Degradation of recycled high-impact polystyrene .Simulation by reprocessing and thermo-oxidation. Polymer Degradation and Stability 2006; 91: 2163-2170.

9. Vilaplana F, Karlsson S, Ribes-Greus A. Changes in the micro-structure and morphology of high-impact polystyrene subjected to multiple processing and thermo-oxidative degradation. European Polymer Journal 2007; 43: 4371-4381.

10. Badía JD, Vilaplana F, Karlsson S, Ribes-Greus A. Thermal analysis as a quality tool for assessing the influence of thermo-mechanical degradation on recycled poly(ethylene terephthalate). Polymer Testing 2009; 28: 169-175.

11. La Mantia F, Vinci M. Recycling poly(ethylene terephthalate). Polymer Degradation and Stability 1994; 45: 121-125.

12. Torres N, Robin JJ, Boutevin B. Study of thermal and mechanical properties of virgin and recycled poly(ethylene terephthalate) before and after injection molding. European Polymer Journal 2000;36: 2075-2080.

13. Badía JD, Strömberg E, Ribes-Greus A, Karlsson S. A statistical design of experiments for optimizing the MALDI-TOF-MS sample preparation of polymers. An application in the assessment of the thermo-mechanical degradation mechanisms of poly(ethylene terephthalate). Analytica Chimica Acta 2011; 692: 85-95.

14. Badía JD, Strömberg E, Karlsson S, Ribes-Greus A. The role of crystalline, mobile amorphous and rigid amorphous fractions on the performance of recycled poly(ethylene terephthalate) (PET). Polymer Degradation and Stability 2012; 97: 98-107

15. Touati N, Kaci M, Bruzaud S, Grohens Y. The effects of reprocessing cycles on the structure and properties of isotactic polypropylene/cloisite 15A nanocomposites. Polymer Degradation and Stability 2011; 96: 1064-1073.

16. Remili C, Kaci M, Benhamida A. Bruzaud S, Grohens Y. The effects of reprocessing cycles on the structure and properties of polystyrene/Cloisite15A nanocomposites. Polymer Degradation and Stability 2011; 96: 1489-1496.

17. Nait-Ali L K, Colin X, Bergeret A. Kinetic analysis and modelling of PET macromolecular changes during its mechanical recycling by extrusion. Polymer Degradation and Stability 2011; 96: 236-246.

18. Zenkiewicz M, Richert J, Rytlewsky P, Moraczewski K, Stepczynska M, Karasiewicz T. Characterisation of multi-extruded poly(lactic acid). Polymer Testing 2009; 28: 412-418.

19. Pillin I, Montrelay N, Bourmaud A, Grohens Y. Effect of thermo-mechanical cycles on the physico-chemical properties of poly(lactic acid). Polymer Degradation and Stability 2008; 93: 321-328.

20. Badia J D , Strömberg E, Ribes-Greus A, Karlsson S. Assessing the MALDI-TOF MS sample preparation procedure to analyze the influence of thermo-oxidative ageing and thermo-mechanical degradation on poly (lactide). European Polymer Journal 2011; 47: 1416-1428.

21. Badia J D, Santonja-Blasco L, Martínez-Felipe A, Ribes-Greus A. A methodology to assess the energetic valorization of bio-based polymers from the packaging industry: Pyrolysis of reprocessed polylactide. Manuscript.

22. Badia J D, Santonja-Blasco L, Martínez-Felipe A, Ribes-Greus A. An assessment on the combustion process of reprocessed polylactide. Manuscript.

23. Carrasco F; Pagès P; Gámez-Pérez J; Santana OO, Maspoch ML. Processing of poly(lactic acid): Characterization of chemical structure, thermal stability and mechanical properties. Polymer Degradation and Stability 2010; 95: 116-125.

24. Carrasco F, Pagès P, Gámez-Pérez J, Santana OO, Maspoch ML. Kinetics of the thermal decomposition of processed poly(lactic acid). Polymer Degradation and Stability 2010;95:2508-2514

25. Södergård A, Stolt M. Properties of lactic acid based polymers and their correlation with composition. Progress in Polymer Science 2002; 27: 1123-1163.

26. Natureworks®, PLA Polymer 2002D. Data Sheet, Natureworks LLC (2005), Available form: http://www.natureworksllc.com [accessed 12.09.2011]

27. ISO 527-2: Plastics -- Determination of tensile properties -- Part 2: Test conditions for moulding and extrusion plastics. 1993.

28. Santonja-Blasco L, Moriana R, Badía JD, Ribes-Greus A. Thermal analysis applied to the characterization of degradation in soil of polylactide: I. Calorimetric and viscoelastic analyses. Polymer Degradation and Stability 2010; 95: 2185-2191.

29. ISO 291. Plastics - standard athmospheres for conditioning and testing. 1997

30. ISO 179-1 Plastics -- Determination of Charpy impact properties -- Part 1: Non-instrumented impact test. 2010.

31. Kister G, Cassanas G, Vert, M. Effects of morphology, conformation and configuration on the IR and Raman spectra of various poly(lacitc acid)s. Polymer 1998; 39: 267-272.

32. 1628-1:2009, ISO. Determination of the viscosity of polymers in dilute solution using capillary viscometers -- Part 1: General principle.

33. Spinu M, Jackson C, Keating M Y, Gardner K H. Material Design in Poly(Lactic Acid) Systems: Block Copolymers, Star Homo- and Copolymers, and Stereocomplexes. Journal of Macromolecular Science, Pure Applied Chemistry 1996; 33: 1497-1530.

34. Levenberg K. A method for solution of certain non-linear problems in least squares. Quaterly of Applied Mathematics 1944; 2: 164-168.

35. Marquardt D. W. An algorithm for the least-squares estimation of non-linear parameters. SIAM Journal of Applied Mathematics, 1963; 11: 431-441.

36. ISO 11357-2 Plastics. Differential Scanning Calorimetry. Part 2- Determination of the glass transition. 1999.

37. Fox T.G., Flory P.J. Second-order transition temperatures and related properties of polystyrene, Journal of Applied Physics 1950; 21: 581–591

38. Pantani R, De Santis F, Sorrentino A, De Maio F, Titomanlio G. Crystallization kinetics of virgin and processed poly(lactic acid). Polymer Degradation and Stability 2010; 95: 1148-1159.

39. Yasuniwa M, Tsubakihara S, Sugimoto Y, Nakafuku C. Thermal analysis of the double-melting behavior of poly(l-lactic acid). Journal of Polymer Science: Part B: Polymer Physics 2004; 42: 25-32.

40. Pan P, Kai W, Zhu B, Dong T, Inoue Y. Polymorphous crystallization and multiple melting behavior of poly(L-lactide): Molecular weight dependence. Macromolecules 2007; 40: 6898-6905.

41. Alves NM, Mano JF, Gómez-Ribelles JL. Molecular mobility in polymers studied with thermally stimulated recovery. II. Study of the glass transition of a semicrystalline PET and comparison with DSC and DMA results. Polymer 2002;43: 3627-3633.

42. Zuza E, Ugartemendia JM, López A, Meaurio E, Lejardi A, Sarasua JR. Glass transition behavior and dynamic fragility in polylactides containing mobile and rigid amorphous fractions. Polymer 2008; 49: 4427-4432.

43. Arnoult M, Dargent E, Mano JF. Mobile amorphous phase fragilty in semi-crystalline polymers: comparison of PET and PLLA. Polymer 2007;48: 1012-1019.

44. Yang S L, Wu Z H, Yang M B. Thermal and mechanical properties of chemical crosslinked polylactide (PLA). Polymer testing 2008; 27: 957-963.

45. Godard M.E., Saiter J.M. Fragility and non-linearity in polymethyl(α-n-alkyl)acrylates. Journal of Non-Crystalline Solids 1998; 23: 635-639.

46. Saiter A, Hess M, D'Souza NA, Saiter JM. Entropy and fragility in vitreous polymers. Polymer 2002; 43: 7497-7504.

47. Vogel H. The temperature dependence law of the viscosity of fluids. Phys Z 1921; 22: 645–646.

48. Fulcher G.S. Analysis of recent measurements of the viscosity of glasses. Journal of the American

Ceramic Society 1925; 8: 339-355.

49. Tammann G, Hesse G. The dependence of viscosity upon temperature of supercooled liquids. Z

Anorg Allg Chem. 1926; 156: 245-257.

50. Vilgis T.A.. Strong and fragile glasses: A powerful classification and its consequences. Physical

Review B 1993; 47 2882-2885.

51. Mijovic J, Sy J W. Molecular dynamics during crystallization of poly(l-lactic acid) as studied by broad-band dielectric relaxation spectroscopy. Macromolecules 2002; 35: 6370-6376.

52. Kunal K, Robertson C. G, Pawlus S, Hahn S. F, Sokolov A. P. Role of Chemical Structure in

Fragility of Polymers: A Qualitative Picture. Macromolecules 2008; 41: 7232-7238.

Table 1. Evolution of DSC parameters

Material	T_G (ºC)	T_{CC0} (ºC)	T_{CC} (ºC)	Δh_{CC} ($J \cdot g^{-1}$)	Δh_M ($J \cdot g^{-1}$)
VPLA	57,2 ± 0,1	106,2 ± 1,7	123,5 ± 0,2	2,21 ± 0,01	2,19 ± 0,04
RPLA-1	56,7 ± 0.1	105,6 ± 0,3	117,3 ± 0,3	23,37 ± 0,14	23,83 ± 0,67
RPLA-2	56,5 ± 0.2	102,0 ± 0,1	110,2 ± 0,4	28,52 ± 0,34	29,77 ± 1,70
RPLA-3	56,7 ± 0,3	101,2 ± 0,6	109,1 ± 1,0	28,32 ± 0,60	27,33 ± 0,97
RPLA-4	56,8 ± 0,1	100,1 ± 0,3	107,3 ± 0,5	27,41 ± 0,51	26,94 ± 0,52
RPLA-5	56,6 ± 0,1	99,6 ± 0,2	106,4 ± 0,1	28,53 ± 0,73	28,31 ± 1,04

Table 2. Evolution of parameters drawn from DMTA characterization

	Storage modulus				Loss modulus				
Material	$\Delta E'_{GR}$ (Mpa)	$\Delta E'_{RC}$ (Mpa)	$\Delta T'_{RP}$ (ºC)	$\Delta T'_{RC}$ (ºC)	$\Delta E''_{0}$ (Mpa)	$\Delta E''_{GR}$ (Mpa)	$\Delta E''_{RC}$ (Mpa)	$\Delta T''_{GR}$ (ºC)	$\Delta T''_{RC}$ (ºC)
VPLA	235,49 ± 3,50	19,23 ± 1,44	20,5 ± 3,9	13,5 ± 1,4	62,12 ± 4,99	64,33 ± 4,61	1,30 ± 1,33	24,7 ± 1,5	18,4 ± 2,6
RPLA-1	496,67 ± 4,40	28,82 ± 3,02	14,0 ± 3,4	7,7 ± 0,9	89,85 ± 3,23	94,52 ± 3, 29	1,99 ± 1,55	21,9 ± 0,9	9,7 ± 1,5
RPLA-2	612,05 ± 5,89	46,96 ± 6,81	11,2 ± 3,4	6,7 ± 0,9	131,00±8,16	137,29 ± 7, 06	2,68 ± 1,77	19,4 ± 1,0	8,9 ± 2,2
RPLA-3	397,65 ± 5,19	28,84 ± 4,19	11,1 ± 2,8	6,1 ± 0,9	85,33±5,79	89,43 ± 5,37	1,61 ± 2,30	18,3 ± 1,2	7,9 ± 1,3
RPLA-4	381,57 ± 4,29	28,33 ± 5,39	10,2 ± 3,6	5,8 ± 1,0	84,00±3,50	88,17 ± 2,90	1,92 ± 1,28	19,1 ± 1,5	7,5 ± 1,6
RPLA-5	400,03 ± 9,10	30,16 ± 5,33	9,9 ± 3,7	6,0 ± 0,7	86,57±4,02	90,57 ± 3,47	1,77 ± 2,64	18,8 ± 1,5	7,3 ± 1,2

Table 3. Results of fitting the viscoelastic behaviour to VFTH model. Fragility parameters: D, B, m.

Material	VFTH				
	R^2	T_{VFTH} (ºC)	D	B (K)	m
VPLA	0,994	15,8 ± 0,4	5,47 ± 0.10	1581	127
RPLA-1	0,972	19,3 ± 2,1	5,55 ± 0,31	1622	143
RPLA-2	0,973	22,0 ± 2,1	5,65 ± 0,92	1655	156
RPLA-3	0,961	25,1 ± 0,9	4,36 ± 0,53	1292	120
RPLA-4	0,964	26,0 ± 1,7	4,32 ± 0,42	1284	120
RPLA-5	0,953	26,1 ± 2,0	4,33 ± 0,31	1283	122

CAPTIONS TO FIGURES

Figure 1. SEM pictures of (a) VPLA and (b) RPLA-5.

Figure 2. Results from tensile and impact testing: (a) Young Modulus and Impact value; (b) Stress and Strain at break.

Figure 3. FT-IR analysis: (a) FT-IR spectra of virgin and fifth reprocessed PLA; (b) evolution of the carbonyl region; (c) variation of the hydroxyl region; (d) changes in functional indexese

Figure 4. Variation of intrinsic viscosity and molar mass throughout the injection steps. Insert: Detail of calculation of Huggins and Kraemer plots for the case of VPLA.

Figure 5. Evolution of the heating DSC thermograms for VPLA and RPLA-i (i:1-5)

Figure 6. Results of the partial area study after deconvolution of the melting region of the DSC scans.

Figure 7. DMTA spectra of VPLA at 1Hz: (upper) loss modulus; (lower) storage modulus

Figure 8. Evolution of storage (lower) and loss (upper) moduli at 1 Hz.

Figure 9. Evolution of apparent activation energy associated to the glass-rubber relaxation and coefficient of free volume.

FIGURE 1

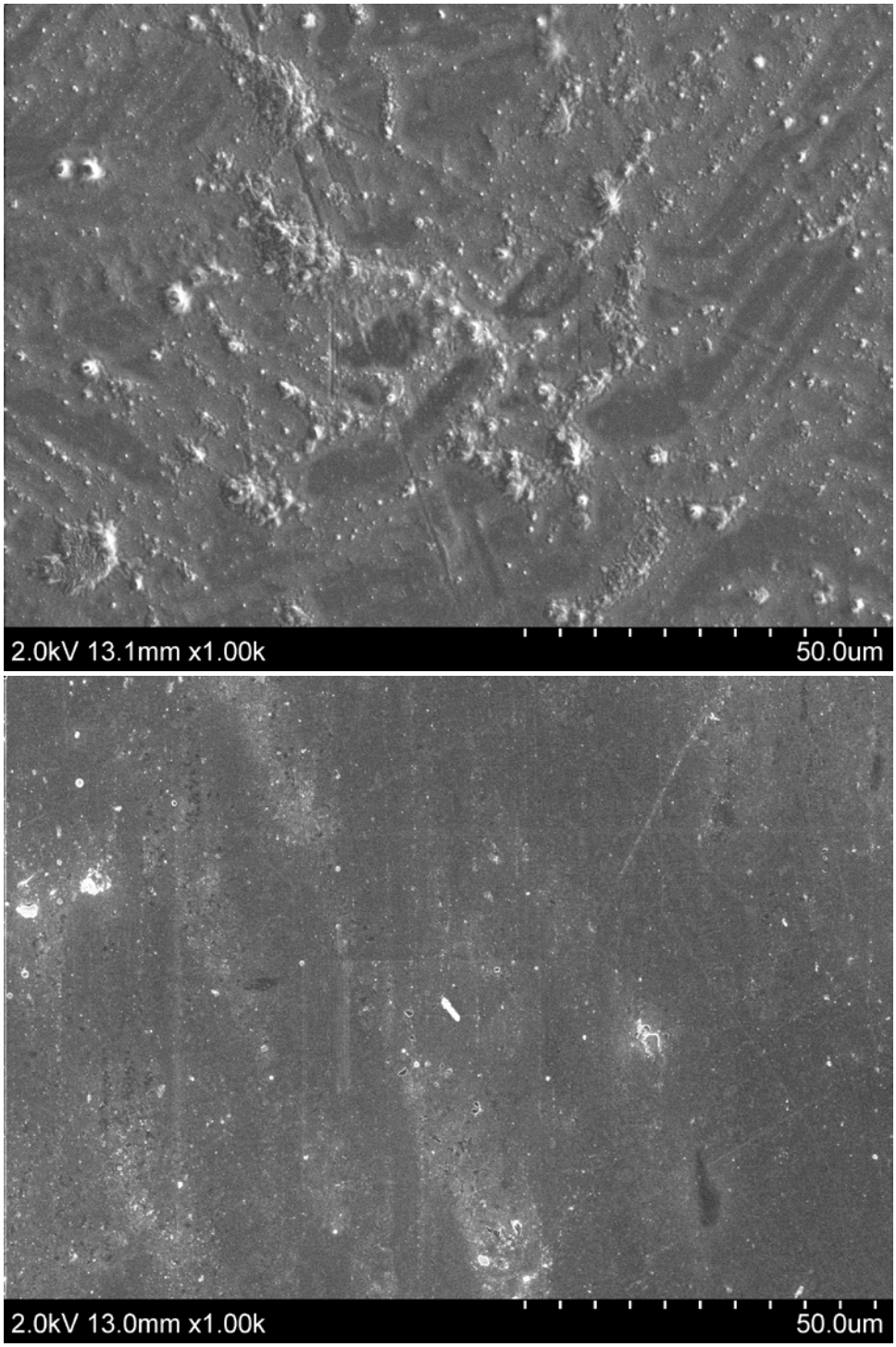

Badia, J. D., Strömberg, E., Karlsson, S., & Ribes-Greus, A. (2012). Material valorisation of amorphous polylactide. Influence of thermo-mechanical degradation on the morphology, segmental dynamics, thermal and mechanical performance. *Polymer degradation and stability*, *97*(4), 670-678.

FIGURE 2

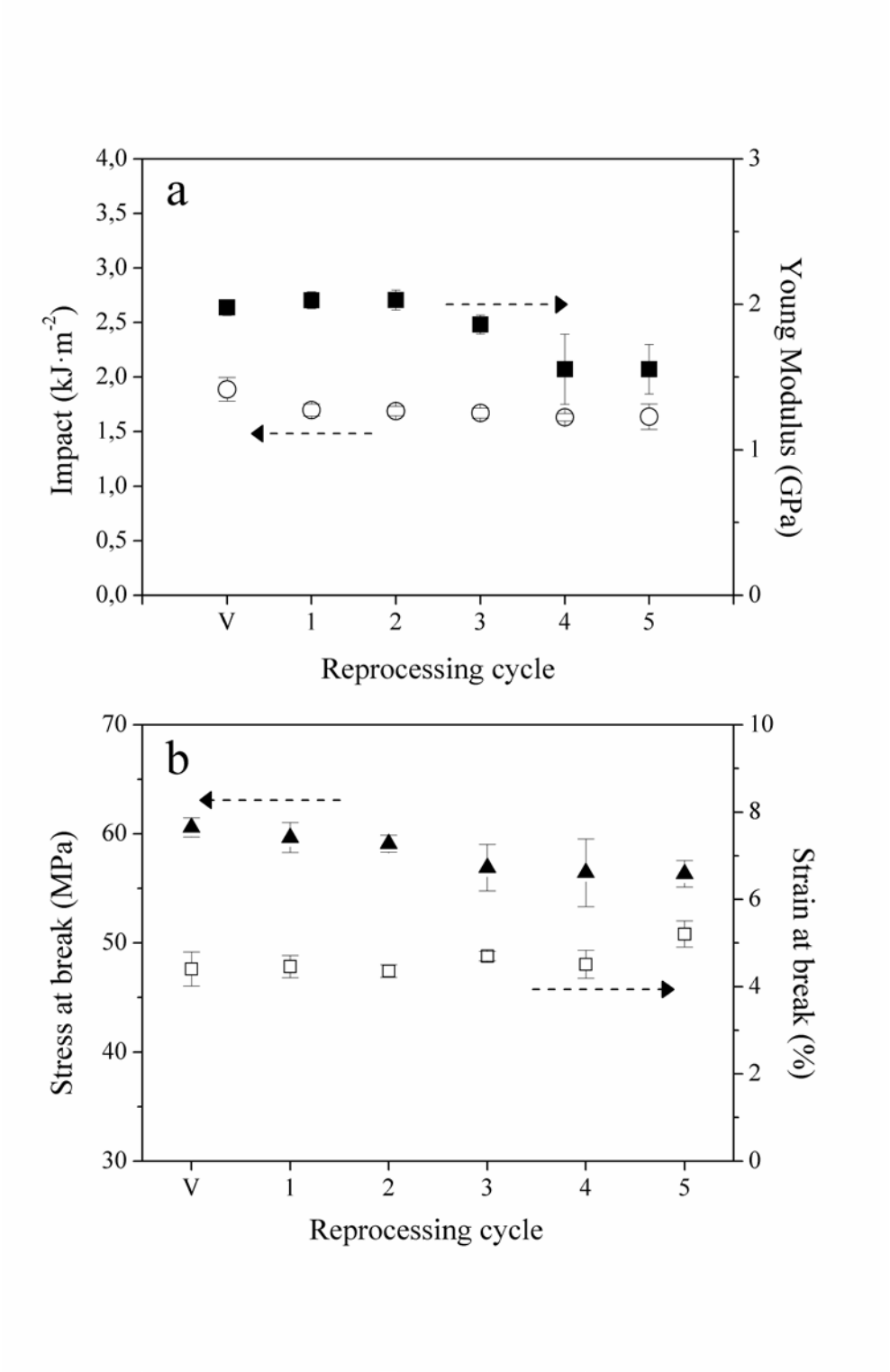
a
Impact (kJ·m-2)
Young Modulus (GPa)
Reprocessing cycle
V
1
2
3
4
5
b
Stress at break (MPa)
Strain at break (%)
Reprocessing cycle

FIGURE 3

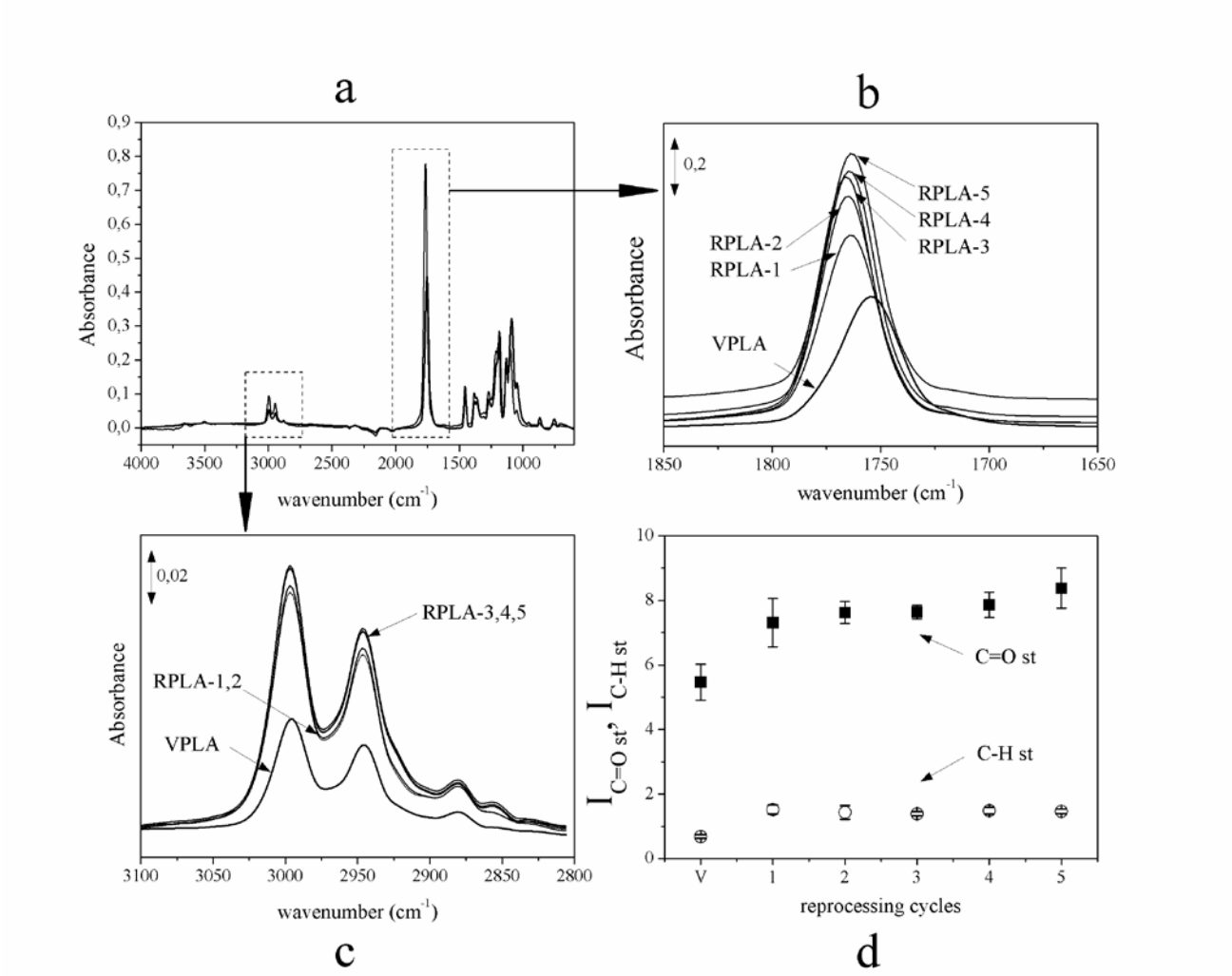
a
b
c
d
Absorbance
wavenumber (cm-1)
0,2
0,02
RPLA-5
RPLA-4
RPLA-3
RPLA-2
RPLA-1
VPLA
RPLA-3,4,5
RPLA-1,2
C=O st
C-H st
I C=O st, I C-H st
reprocessing cycles

FIGURE 4

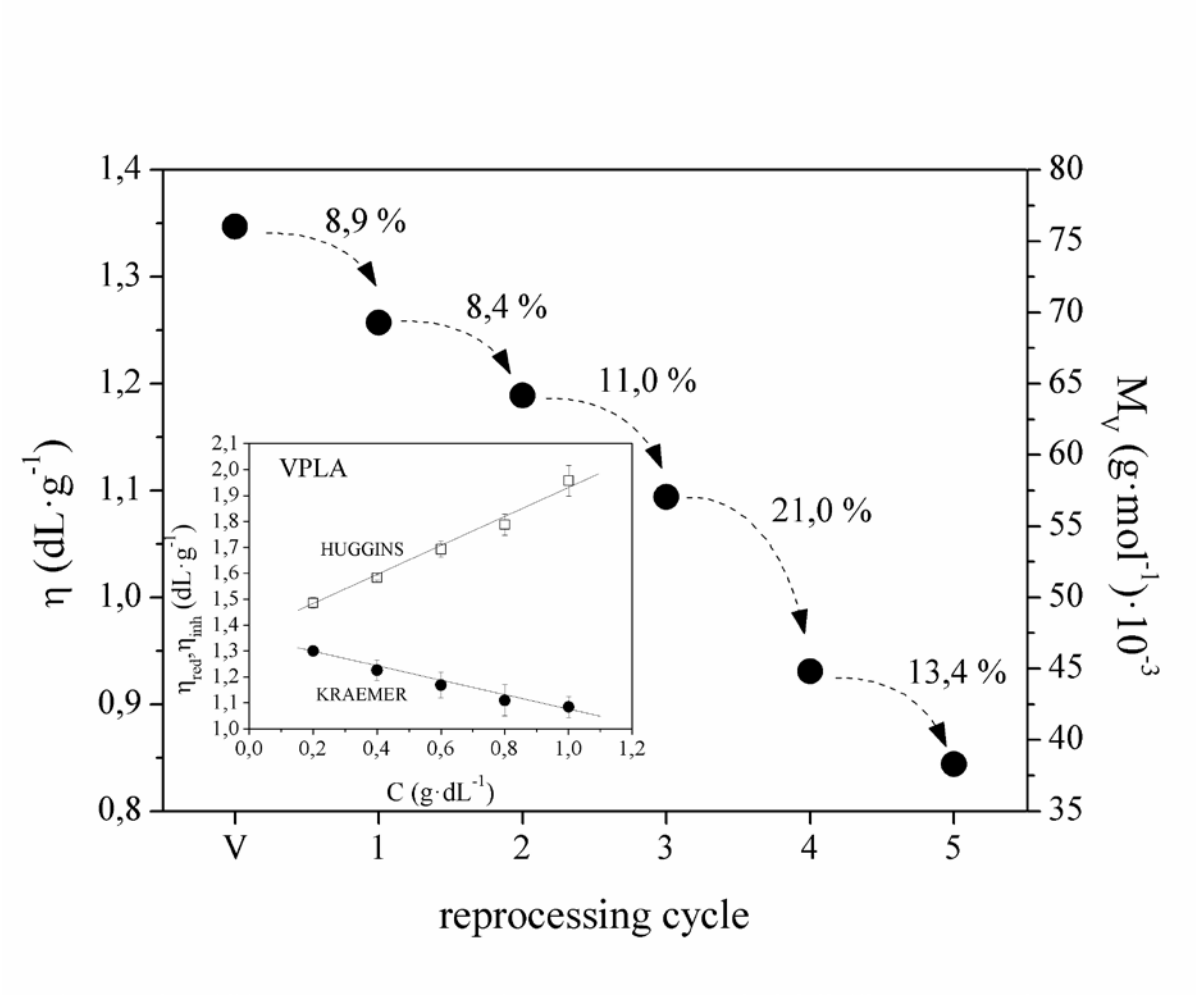
8,9 %
8,4 %
11,0 %
21,0 %
13,4 %
VPLA
HUGGINS
KRAEMER
η_{red}, η_{inh} (dL·g^{-1})
C (g·dL^{-1})
η (dL·g^{-1})
M_V (g·mol^{-1})·10^{-3}
V
reprocessing cycle

FIGURE 5

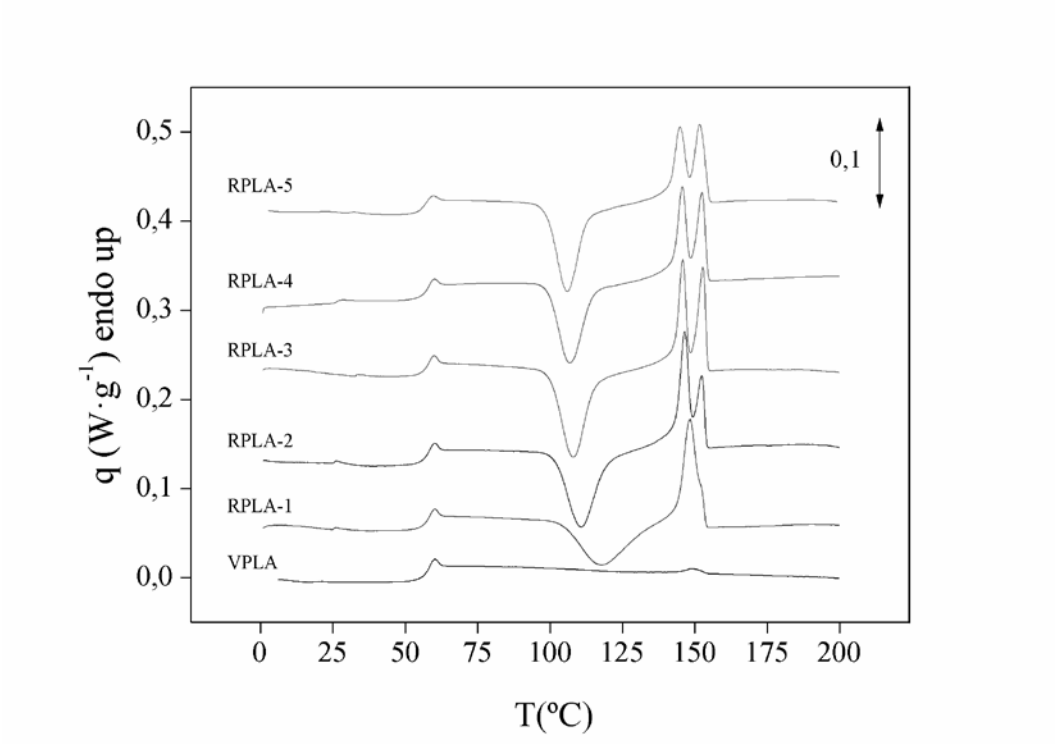
0,5
0,4
0,3
0,2
0,1
0,0
q (W·g-1) endo up
0,1
RPLA-5
RPLA-4
RPLA-3
RPLA-2
RPLA-1
VPLA
0
25
50
75
100
125
150
175
200
T(ºC)

FIGURE 6

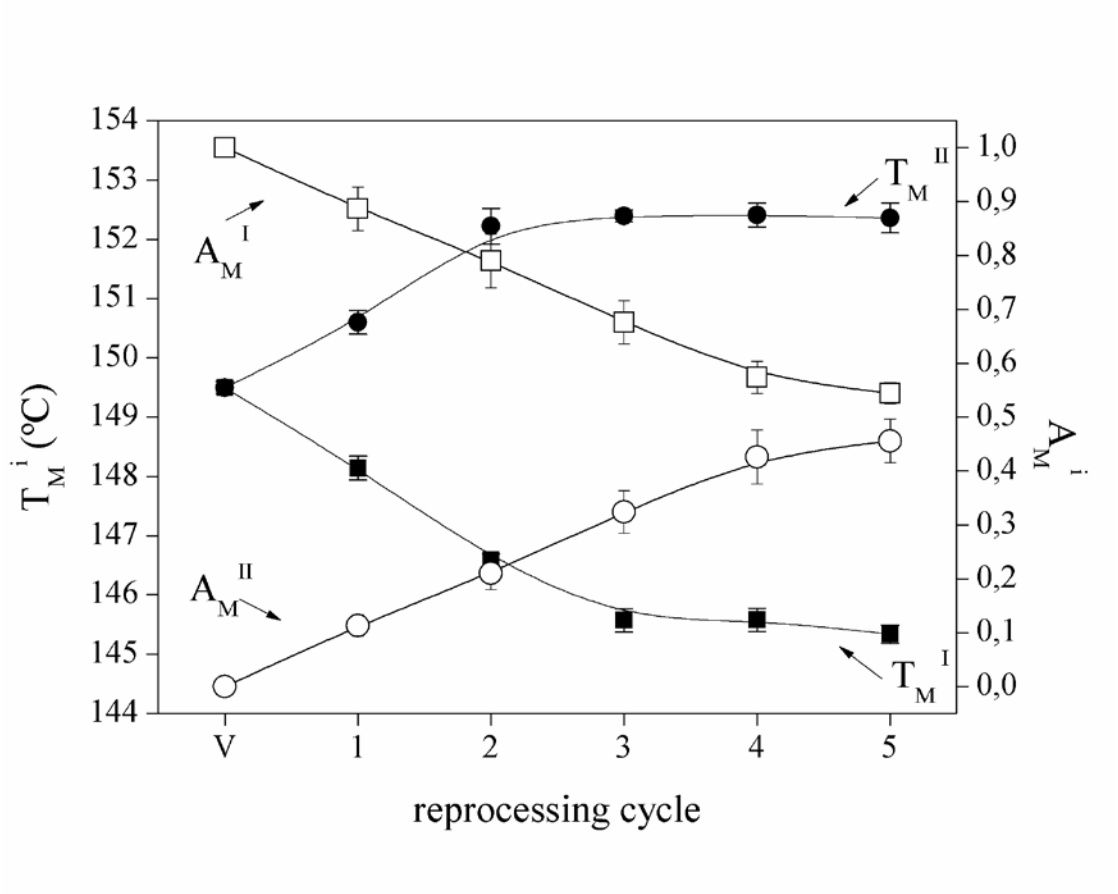
154
153
152
151
150
149
148
147
146
145
144
1,0
0,9
0,8
0,7
0,6
0,5
0,4
0,3
0,2
0,1
0,0
V
1
2
3
4
5
reprocessing cycle
T_M^i (°C)
A_{M_i}
T_M^{II}
T_M^I
A_M^I
A_M^{II}

FIGURE 7

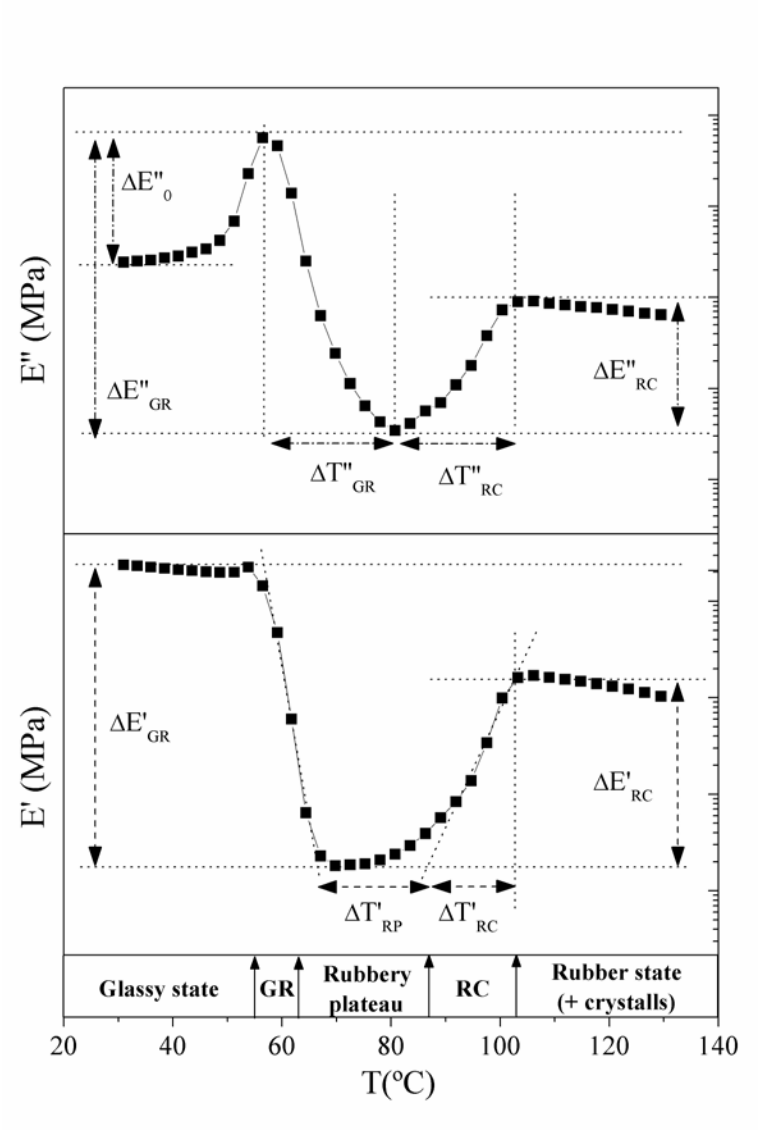
E'' (MPa)
ΔE''0
ΔE''GR
ΔE''RC
ΔT''GR
ΔT''RC
E' (MPa)
ΔE'GR
ΔE'RC
ΔT'RP
ΔT'RC
Glassy state
GR
Rubbery plateau
RC
Rubber state (+ crystalls)
20
40
60
80
100
120
140
T(ºC)

FIGURE 8

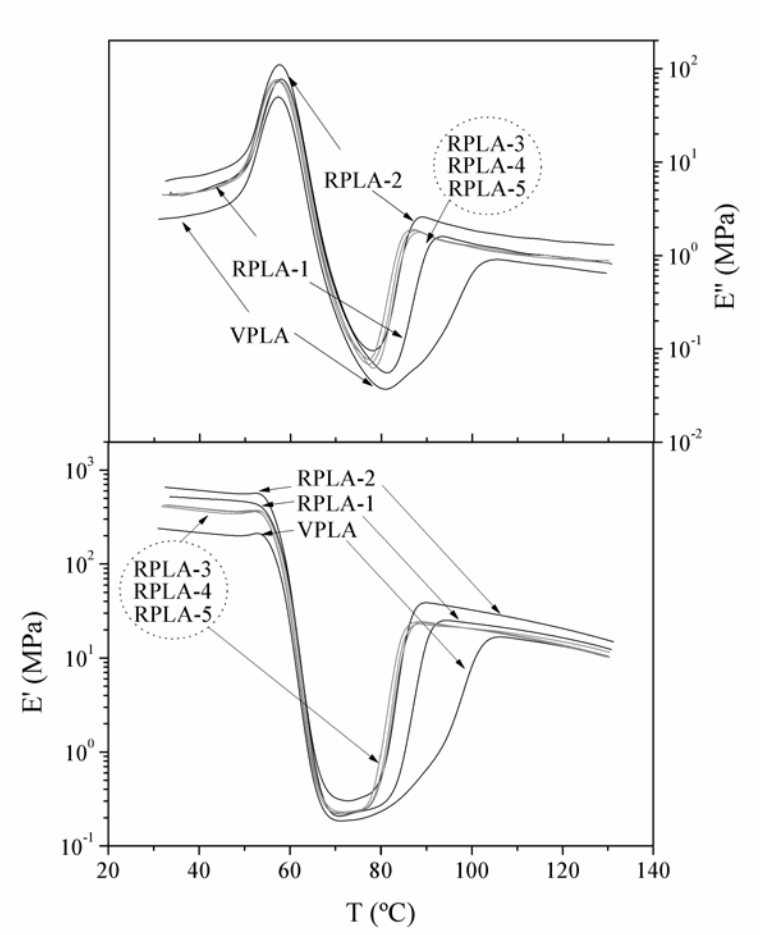

FIGURE 9

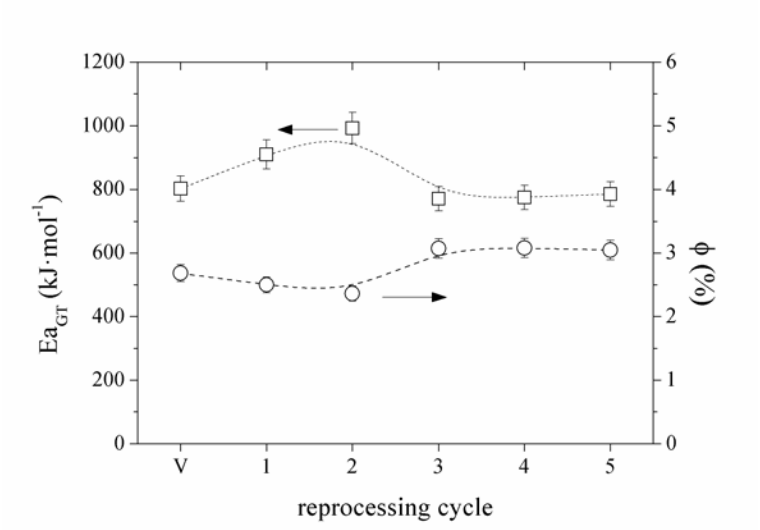
1200
1000
800
600
400
200
0
6
5
4
3
2
1
0
V
1
2
3
4
5
reprocessing cycle
Ea_{GT} (kJ·mol^{-1})
ϕ (%)

Badia, J. D., Strömberg, E., Karlsson, S., & Ribes-Greus, A. (2012). Material valorisation of amorphous polylactide. Influence of thermo-mechanical degradation on the morphology, segmental dynamics, thermal and mechanical performance. *Polymer degradation and stability*, *97*(4), 670-678.

Shortly, a fragile glass-former experiences a dramatic loss of properties (rheological, mechanical…) throughout a specific short temperature interval, such as the glass-rubber relaxation, while a strong glass-former maintains its properties without any significant change. The relaxation of strong systems is generally found to be Arrhenius-like, whereas for fragile systems, it is remarkably non-Arrhenius [45-46] and describable by a Vogel-Fulcher-Tamman-Hesse (VFTH) behaviour [47-49] , as shown in Eq. (1)

$$\tau(T) = \tau(T) = \tau_0 \cdot exp\left(\frac{B}{T - T_{VFTH}}\right) = \tau_0 \cdot exp\left(\frac{D \cdot T_{VFTH}}{T - T_{VFTH}}\right)$$

(1)

, where τ are the relaxation times (s), that is $(2 \cdot \pi \cdot f)^{-1}$, and f is the linear frequency of the DMTA tests, τ_0 is a time reference scale, and B (K) and T_{VFTH} (K) are positive parameters specific to the material. T_{VFTH} typically appears 40-60 K below the T_G. It is common to rewrite the parameter B into $B = D \cdot T_{VFTH}$, where D is a dimensionless factor termed as fragility or strength parameter. Qualitatively, D is related to the topology of the theoretical potential energy surface of the system, where fragile systems ($D \leq 6$) present high density of energy minima, contrarily to strong systems ($D \geq 15$) which present lower density. As well, the so-called fragility index m permits an assessment of the deviation of $\tau(T)$ from the Arrhenius behavior of polymers. It varies between two limiting values of 16 and ≥ 200 for strong and fragile glass-formers, respectively [50], and can be obtained by the following expression:

$$m = \left.\frac{d \log(\tau)}{d(T_G/T)}\right|_{T=TG} = \left.\frac{B \cdot T}{\ln(10) \cdot (T_G - T_{VFTH})^2}\right|$$

(2)

In order to study the effects of reprocessing on the dynamic fragility of PLA, the relationship of τ with the T_P from the different loss tangent spectra were fitted to the VFTH model, which results with linear correlation R^2 coefficients higher than 0,950 are gathered in **Table 3**, along with the fragility parameters D, B and m. VPLA showed fragile glass-former performance, in agreement with other studies performed on fully amorphous PLA [51]. Up to the second recyclate, PLA became more fragile. Afterwards, there was

a change in the variation trend. These results were in agreement with the evolution shown by the mechanical stresses, as can be seen in **Table 2.**

The influence of the chemical structure of polymers on their fragility was discussed with detail by *Sokolov et al*. [52]. The changes can be ascribed to the mobility of chains, both physically or chemically, which in turn will affect the cooperative movement and the packing efficiency. An increase in fragility implies higher chain cooperativity and vice versa. Thus, the subsequent calculation of the activation energies related to the glass-rubber relaxation Ea_{GT}, or the free volume coefficient ϕ obtained by means of Eqs. (3) and (4) could picture the change in cooperative movement due to thermo-mechanical degradation.

$$Ea_{GT} = R \cdot \frac{d\ln\tau}{d\left({}^{1}/_{T}\right)} = \frac{R \cdot B}{\left(1 - \frac{T_{VFTH}}{T}\right)^{2}} \quad (3)$$

(3)

$$\phi = \frac{(T - T_{VFTH})}{B} \quad (4)$$

(4)

As can be seen in **Figure 9**, both Ea_{GT} and ϕ displayed a logical contrary behaviour. After the second recyclate, the free volume considerably increased (~20 %) which may promote the liability of gases to permeate through the packing defects of the polymer in packaging applications therefore reducing the second-life performance of PLA for similar purposes.

Table 3-Figure 9

3.5. Summary of results

The thermo-mechanical degradation inherent to mechanical recycling induced chain scission reactions releasing mainly carboxyl species which remained amorphous regardless the number of injection cycles. Consequently, the viscous molar mass decayed. Chain scission could be followed by monitoring the col-crystallization induced during the calorimetric experiments, in terms of a decrease of the cold-crystallization temperature and an increase in the cold-crystallization enthalpy. The tendency of the bimodal melting

endotherm to change towards the peak at lower temperatures $T_M{}^I$, along with the stabilization of the partial melting temperature just after the second reprocessing step may indicate that a limiting length of scissored chain was attained. The arrangement of the scissored chains in the amorphous matrix was noticeably influent from the second reprocessing step on. The reduction of chain length during further injection cycles might had affected the mobility of chains leaving more free volume, thus easing the glass-rubber relaxation with lower mechanical stresses and activation energies, since the dynamic fragility was reduced. In connection, the less efficient packing of PLA reprocessed more than 2 times could explain the reduction of the Young Modulus and stress at break found in the study of the macroscopic mechanical properties.

4. Conclusions

Polylactide (PLA) submitted to in-plant recycling simulation underwent thermo-mechanical degradation which modified its structure and morphology and induced changes on its thermal and mechanical properties.

Despite non-significant changes were drawn from the observation of the functional groups of PLA, a remarkable reduction in molar mass was found, due to chain scission processes After each of the 5 applied reprocessing steps, PLA remained amorphous in the glassy state. However, the study of the calorimetric thermograms showed the apparition of a cold-crystallization phenomenon, which was favoured by the presence of shorter PLA chains due to chain scission processes, particularly after the second reprocessing cycle. This fact was also confirmed by monitoring the melting endotherm. The rearrangement of cut chains into the amorphous matrix offered more free volume which favoured the mobility of chains throughout the glass-rubber relaxation and reduced the dynamic fragility of reprocessed PLA. In macroscopic terms, it was related to a decay in elastic modulus and stress at break, as well as it influenced the surface heterogeneity.

As a whole, all assessed properties showed a significant loss of PLA performance after the application of the second reprocessing step, thus suggesting a sort of threshold to be recovered by further mechanical recycling.

Acknowledgements

The authors would like to acknowledge the Spanish Ministry of Science and Innovation for the financial support through the Research Project UPOVCE-3E-013 and for the funding of a predoctoral research position to J.D. Badía by means of the FPU program conceded by the Spanish Ministry for Education. The authors acknowledge the financial support of the Generalitat Valenciana through the ACOMP/2011/189. Universitat Politècnica de València (UPV, Spain) is thanked for additional support through the PAID 05-09-4331 program and Royal Institute of Technology (KTH, Sweden) is thanked for additional. Mr. Enrique Benavent at AIMPLAS is acknowledged for taking care of processing the material. Mr. Peter Kaali at KTH is thanked for carrying out impact tests and Mrs. Sevil Atari Jabarzadeh at KTH for helping with SEM analysis. Mrs. L. Santonja-Blasco at UPV is thanked for endless and enjoyable discussions.